

# BrainNetVis: Analysis and Visualization of Brain Functional Networks

Vassilis Tsiaras, Dimitris Andreou and Ioannis G. Tollis

**Abstract**—BrainNetVis is an application, written in Java, that displays and analyzes synchronization networks from brain signals. The program implements a number of network indices and visualization techniques. We demonstrate its use through a case study of left hand and foot motor imagery. The data sets were provided by the Berlin BCI group. Using this program we managed to find differences between the average left hand and foot synchronization networks by comparing them with the average idle state synchronization network.

## I. INTRODUCTION

One of the major issues in neuroscience is to describe how different brain areas communicate with each other during perception, cognition, action as well as during spontaneous activity in the default or resting state. Friston [1] defined functional connectivity as the statistical dependence between the activations of distinct and often well separated neuronal populations. Network models and graph theory provide a common framework for describing functional connectivity. In this paper we present a software tool, called BrainNetVis, for the analysis and visualization of brain functional networks. We demonstrate the tool and discuss the implemented network measures and visualization techniques using EEG data from BCI IV competition and working at sensors space. However the tool is not restricted to sensors space since the input consists of synchronization matrices. Therefore our discussion is valid for the generators space as well.

## II. MATERIALS AND SIGNAL PROCESSING

### A. Experimental Setup

We use motor imagery (without feedback) data sets provided by the Berlin BCI group for the Brain Computer Interface (BCI) competition IV [2]. Four of data sets 1, the a, b, f and g, were recorded from four healthy subjects. Brain activity was recorded with multi-channel EEG amplifiers using 59 channels band-pass filtered between 0.05 and 200 Hz and sampled at 1000 Hz. For each subject two classes of motor imagery were selected: left hand (L), and foot (F) (side chosen by the subject; optionally also both feet).

This research was supported in part by the European Commission FP7 ‘Virtual Physiological Human Network of Excellence’ grant (project n° 223920).

V. Tsiaras, D. Andreou and I. G. Tollis are with the Institute of Computer Science, Foundation for Research and Technology, Heraklion 71110, Greece {tsiaras, andreou, tollis}@ics.forth.gr

V. Tsiaras and I. G. Tollis are with the Department of Computer Science, University of Crete, Heraklion, Crete, GR-71409 Greece {tsiaras, tollis}@csd.uoc.gr

### B. Power Spectral Density Estimation

The multichannel EEG was filtered using the Common Spatial Patterns (CSP) spatial filter and then the Power Spectral Density (PSD) was calculated using Welch’s method. The CSP [3] is a technique to analyze multi-channel data based on recordings from two classes. Let  $\Sigma^{(L)} \in \mathbb{R}^{n \times n}$  and  $\Sigma^{(F)} \in \mathbb{R}^{n \times n}$  be the estimates of the covariance matrices of the (assumed to be zero mean) EEG signal in the two classes (left hand and foot imagination):

$$\Sigma^{(c)} = \frac{1}{|\mathcal{I}_c|} \sum_{i \in \mathcal{I}_c} X_i X_i^T, \quad c \in \{L, F\}$$

where  $\mathcal{I}_c$  is the set of indices corresponding to trials belonging to class  $c \in \{L, F\}$ . By extracting the eigenvectors and eigenvalues from  $\Sigma = \Sigma^{(L)} + \Sigma^{(F)} = U_0 \Lambda U_0^T$  we can calculate the spatial factors matrix  $Q = U_0 \Lambda^{1/2}$  and the whitening matrix  $P = \Lambda^{-1/2} U_0^T$ . Then we calculate matrices  $S^{(L)} = P \Sigma^{(L)} P^T$  and  $S^{(F)} = P \Sigma^{(F)} P^T$  and their eigenvalues and eigenvectors:  $S^{(L)} = U \Lambda^{(L)} U^T$  and  $S^{(F)} = U \Lambda^{(F)} U^T$ , where  $\Lambda^{(L)} + \Lambda^{(F)} = I$  and  $\Lambda_{ii}^{(L)} \leq \Lambda_{jj}^{(L)}$  when  $i < j$ . Taking the first  $r$  (resp. last  $r$ ) eigenvectors from  $U$ , we obtain  $U_r \in \mathbb{R}^{r \times n}$  to compute the filtered EEG signal

$$X_r^{(F)} = Q U_r U_r^T P X \quad (\text{resp. } X_r^{(L)} = Q U_r U_r^T P X)$$

### C. Synchronization Measures

Signal segments of duration 4s that correspond to motor imagery or idle state are bandpass filtered using a zero phase forward and reverse Butterworth filter which does not significantly affect the reconstruction of the dynamics of a system [4]. Then for mu and beta frequency bands, the synchronization between all pairs of channels is calculated using a) a non-linear bivariate measure for generalized synchronization and b) partial directed coherence.

1) *A Robust Interdependence Measure (RIM)*: Given two scalar time series  $\{x(t)\}_{t \in \mathbb{T}}$  and  $\{y(t)\}_{t \in \mathbb{T}}$  with  $\mathbb{T} = \{1, \dots, N\}$ , which have been measured from dynamical systems  $X$  and  $Y$ , the dynamics of the systems are reconstructed using delay coordinates [5]

$$\mathbf{x}(t) = [x(t), x(t + \tau), \dots, x(t + (m - 1)\tau)]^T$$

and similarly we reconstruct  $\mathbf{y}(t)$  from  $\{y(t)\}_{t \in \mathbb{T}}$ , with an embedding dimension  $m$  and a delay time  $\tau$  for  $n \in \mathbb{T}' = \{1, \dots, N'\}$ , where  $N' = N - (m - 1)\tau$ .

Let  $r_{t,j}$  and  $s_{t,j}$ ,  $j = 1, \dots, k$ , denote the time indices of the  $k$  nearest Euclidean neighbors of  $\mathbf{x}(t)$  and  $\mathbf{y}(t)$ , respectively. Temporally correlated neighbors are excluded by means of a Theiler correction:  $|r_{t,j} - t| > m \cdot \tau$  and

$|s_{t,j}-t| > m \cdot \tau$ . For each  $t \in \mathbb{T}'$ , the average square distance of  $\mathbf{y}(t)$  to all remaining points in  $\{\mathbf{y}(j)\}_{j \in \mathbb{T}'}$  is given by

$$R_t(Y) = \frac{1}{N' - 1} \sum_{j=1, j \neq t}^{N'} |\mathbf{y}(t) - \mathbf{y}(j)|^2$$

For each  $\mathbf{y}_t$ , the X-conditioned mean squared Euclidean distance is defined as

$$R_t^{(k)}(Y/X) = \frac{1}{k} \sum_{j=1}^k |\mathbf{y}(t) - \mathbf{y}(r_{t,j})|^2$$

Quián Quiroga et al. [6] defined the dependence measure:

$$N(Y/X) = \frac{1}{N'} \sum_{t=1}^{N'} \frac{R_t(Y) - R_t^{(k)}(Y/X)}{R_t(Y)} \quad (1)$$

The measure  $N(X/Y)$  is defined in complete analogy and as interdependence measure between  $X$  and  $Y$  we use the mean value  $(N(X/Y) + N(Y/X))/2$ .

2) *Partial Directed Coherence (PDC)*: Let  $\{\mathbf{x}(t)\}_{t \in \mathbb{N}}$  with  $\mathbf{x}(t) = [x_1(t), \dots, x_n(t)]^T$  be a stationary  $n$ -dimensional time series with mean zero. Then a vector autoregressive model of order  $p$  for  $\mathbf{x}$  is given by

$$\mathbf{x}(t) = \sum_{r=1}^p \mathbf{A}(r)\mathbf{x}(t-r) + \varepsilon(t) \quad (2)$$

where  $\mathbf{A}(r)$  are the  $n \times n$  coefficient matrices of the model and  $\varepsilon(t)$  is a multivariate Gaussian white noise process with covariance matrix  $\Sigma$ . In this model, the coefficients  $A_{ij}(r)$  describe how the present values of  $x_i$  depend linearly on the past values of the components  $x_j$ . In order to provide a frequency domain measure for Granger-causality, Baccala and Sameshima [7] introduced the concept of PDC. This measure is based on the Fourier transform of the coefficient series

$$\bar{\mathbf{A}}(\omega) = I - \sum_{r=1}^p \mathbf{A}(\omega)e^{-i\omega r} \quad (3)$$

More precisely, the PDC from  $x_j$  to  $x_i$  is defined as

$$\pi_{i \leftarrow j}(\omega) = \frac{|\bar{A}_{ij}(\omega)|}{\sqrt{\sum_{l=1}^n |\bar{A}_{lj}(\omega)|^2}} \quad (4)$$

The PDC  $\pi_{i \leftarrow j}(\omega)$  takes values between 0 and 1 and vanishes for all frequencies  $\omega$  if and only if the coefficients  $A_{ij}(r)$  are zero for all  $r = 1, \dots, p$ .

Due to limited number of data samples, PDC was calculated between each pair of channels by taking into account and removing the linear effect of O1 and O2 channels [8].

### III. NETWORK ANALYSIS AND VISUALIZATION

A graph  $G = (V, E)$  defined on a set of vertices  $V = \{v_1, \dots, v_n\}$  and edges  $E = \{e_1, \dots, e_m\}$ , where each edge  $e \in E$  is an ordered or unordered pair of vertices. An ordered pair  $e = (u, v) \in V \times V$  is called a *directed edge*, while an unordered pair  $e = \{u, v\}$ , where  $u, v \in V$ , is called an *undirected edge*. In case  $u = v$ ,  $e$  is called a *self-loop*. In our study we consider *simple* graphs that is graphs without

self-loops and multiple edges. Also the cardinality of  $V$  is denoted by  $n$  (i.e  $n = |V|$ ).

Graphs augmented by edge values are called weighted networks in complex networks literature and valued networks in social networks literature. We prefer the term valued network since in graph theory the term ‘‘weight’’ has been associated with distance, cost and dissimilarity whereas the term ‘‘valued’’ is more general and does not conflict with the notions of synchronization and dependence. The term ‘‘network’’ means a graph that represents something real. A *valued network*  $G = (V, E, \omega)$  consists of a graph with vertex set  $V$  and edge set  $E$  augmented with an edge value function  $\omega : E \rightarrow \mathbb{R}$  that assigns to each edge  $e \in E$  a real value  $\omega(e)$ . Every valued network  $G = (V, E, \omega)$  corresponds to a real  $n \times n$  matrix  $W = (w_{ij})$ ,  $i, j \in \{1, 2, \dots, n\}$ , where  $w_{ij}$  is equal to value  $\omega(e)$  of edge  $e = (v_i, v_j)$  if  $e \in E$ , or to 0 otherwise. If we reserve value 0 to mean the absence of an edge then the correspondence between  $G$  and  $W$  is one-to-one. In this work we consider a subset of valued networks, which we call *synchronization networks*, where edge values are restricted to interval  $(0, 1]$  and interpreted as strength of dependence between vertices.

In synchronization networks higher edge values indicate stronger dependencies. To define the length of an edge we should at least reverse the order of edge values by applying, for example, the inverse function  $g : (0, 1] \rightarrow [1, +\infty)$  with

$$g(x) = \frac{1}{x} \quad (5)$$

We also propose the function  $g : (0, 1] \rightarrow [1, +\infty)$  with

$$g(x) = 1 - \log_2(x) \quad (6)$$

The length of a path from vertex  $u$  to vertex  $v$  is the sum of the lengths of the edges of the path. The shortest path distance from vertex  $u$  to vertex  $v$  is denoted by  $d_G(u, v)$ . If vertex  $v$  is unreachable from vertex  $u$  then  $d_G(u, v) = +\infty$ .

#### A. Vertex Level Measures

The importance of a vertex due to its position in a network is quantified with centrality measures. There is evidence that the importance of a vertex is positively or negatively correlated with the relevance of the vertex to a task.

1) *Strength Centrality*: Strength centrality is the extension of degree centrality to synchronization networks. For each vertex  $v \in V$  is defined as the strength  $s(v)$  of  $v$ . The corresponding normalized measure is:

$$c_S(v) = \frac{1}{n-1} s(v) = \frac{1}{n-1} \sum_{e=\{v,u\} \in E} \omega(e) \quad (7)$$

2) *Shortest-Path Efficiency*: Latora and Marchiori [9] defined efficiency as:

$$c_{Ef}(v) = \frac{1}{n-1} \sum_{u \neq v} \frac{1}{d_G(v, u)} \quad (8)$$

Note that Eq. 8 can also be used for disconnected graphs.

3) *Hubbell's Centrality*: Hubbell [10] suggested a centrality measure based on the solution of a system of linear equations.

$$\mathbf{c} = \alpha W^T \mathbf{c} + \mathbf{e} \quad (9)$$

where  $\mathbf{c} = [c(v_1), c(v_2), \dots, c(v_n)]^T$  is the vector of centralities,  $\mathbf{e} = [e(v_1), \dots, e(v_n)]^T$  is the vector of exogenous factors and  $0 < \alpha < 1/\lambda_1$  where  $\lambda_1$  is the maximum eigenvalue of  $W$ . Equation 9 has the solution:

$$\mathbf{c} = (I - \alpha W^T)^{-1} \mathbf{e} \quad (10)$$

And the normalized Hubbell's centrality is defined as:

$$\mathbf{c}_{HBL} = \mathbf{c} / \|\mathbf{c}\|_p \quad (11)$$

In our work we set

$$e(v) = \frac{\max_{u \in V} (p(u)) - p(v) + \varepsilon}{\max_{u \in V} (p(u)) - \min_{u \in V} (p(u)) + \varepsilon} \quad (12)$$

where  $p(v)$  is the (average) power spectrum at mu or beta band of the corresponding signals and  $\varepsilon$  is a small number.

### B. Network Level Measures

1) *Clustering coefficient*: For a vertex  $v$  the clustering coefficient  $c(v)$  measures the connectivity of its direct neighborhood. The clustering coefficient  $C(G)$  of a graph is the average of  $c(v)$  taken over all vertices. A definition that uses matrix  $W$  was proposed by Zhang and Horvath [11].

$$c_Z(v) = \frac{1}{\max_{i,j} (w_{ij})} \cdot \frac{\sum_{i \neq j \in V \setminus \{v\}} w_{vi} w_{ij} w_{jv}}{\sum_{i \neq j \in V \setminus \{v\}} w_{vi} w_{jv}} \quad (13)$$

where  $\max_{i,j} (w_{ij})$  is a normalizing factor.

2) *Assortativity*: The assortativity coefficient was first defined by Newman [12] for undirected graphs. Leung et al. [13] extended this definition to cover the class of undirected synchronization networks.

$$r = \frac{4H \sum_{\{u,v\} \in E} \omega(u,v) s(u) s(v) - B}{2H \sum_{\{u,v\} \in E} \omega(u,v) (s(u)^2 + s(v)^2) - B} \quad (14)$$

where  $s(v)$  is the strength of vertex  $v$ ,  $H = \sum_{e \in E} \omega(e)$  and  $B = \left[ \sum_{\{u,v\} \in E} \omega(u,v) (s(u) + s(v)) \right]^2$ .

### C. Network Visualization

BrainNetVis allows the user to define the location, label, font, color and size of vertices. Vertices' centrality measures and attributes are visualized through the color of vertices via a colormap. Additionally the implemented measures are displayed in a tabular format on a second window.

Each edge is visualized using shades of grey according to rule  $greyshade = 1 - \omega(e)$ . Alternatively, the edge values define the edge colors via a colormap. Another option is to convert a synchronization network  $G = (V, E, \omega)$  to a graph  $G' = (V, E')$  where  $E' = \{e \in E \mid \omega(e) \geq \theta\}$ , where  $\theta$  is a user defined threshold and then to visualize graph  $G'$  [14].

In order to show the network structure, two network visualization techniques have been implemented. The stress majorization technique of Gansner et al. [15] and the binary stress model of Koren et al. [16].

## IV. RESULTS

For each subject, frequency band and synchronization method we calculated synchronization matrices for every left (L), foot (F) or idle (I) 4 sec period, within the subject's session, that passed the visual check for artifacts. Specifically we calculated more than 80 synchronization matrices for each state (L, F, I) and subject. Then for each subject we calculated the average matrix per state in order to find differences in channels' synchronization between the states. In the following we call L, F and I the average left, foot and idle state networks. The first observation is that functional networks constructed from motor imagery EEG data are dominated by edges that are irrelevant to motor imagery tasks. Especially close-by electrodes are highly synchronized which reflects redundancies in the measurement due to volume conduction rather than brain interaction [17] (see Fig. 1). The second observation is that networks L and F look and are very similar. Network L has clustering and assortativity coefficients 0.51 and 0.126 respectively, while network F has clustering and assortativity coefficients 0.497 and 0.13. These results agree with the results of Calmels et al. [18]. To extract information from networks L and F we compare each one of them with network I. We consider a network that has the same set of vertices as networks L, F and I and has an edge from vertex  $j$  to vertex  $i$  ( $i \leftarrow j$  due to convention of PDC) if and only if  $W_{ij}^{(L)} - W_{ij}^{(I)} > 0$  (resp.  $W_{ij}^{(F)} - W_{ij}^{(I)} > 0$ ). By subtracting network I from network L (resp. F) most noisy edges disappear and in the resulting network one can discern edges related to motor imagery task. For subjects a and g, when networks have been calculated using PDC then the resulting network L minus I has long edges that span both hemispheres and which can be attributed to motor imagery task [8] or to occipital/parietal alpha activity [19]. The long edges are less apparent in network F minus I. When networks have been calculated using the RIM or the magnitude square coherence methods the long edges between hemispheres of network L minus I are present but mixed with other edges that are adjacent to vertices O1 and O2. We repeated this procedure by changing the role of networks I and L (resp. I and F). Namely from network I we subtracted network L (resp. F). In the left (resp. right) graph of Fig. 2 we see that network I minus L (resp. I minus F) has more edges close to the left hand (resp. foot) area of the sensorimotor cortex. There is inter-subject variability since for subjects b and f the long edges across hemispheres appear in networks I minus L and I minus F.

A feature of the tool is that it allows the ranking of vertices according both to their attributes and to their role in a network. In the example of Fig. 2 each vertex is assigned the PSD of the corresponding channel at mu band. In order to improve the signal to noise ratio we spatially filter the multivariate signal using CSP and then we calculate the PSD of each channel at mu band. Then we visualize the PSDs using a colormap and we calculate Hubbell's centrality which combines the PSD with the role of each vertex in a network. We found that the important vertices of network I minus

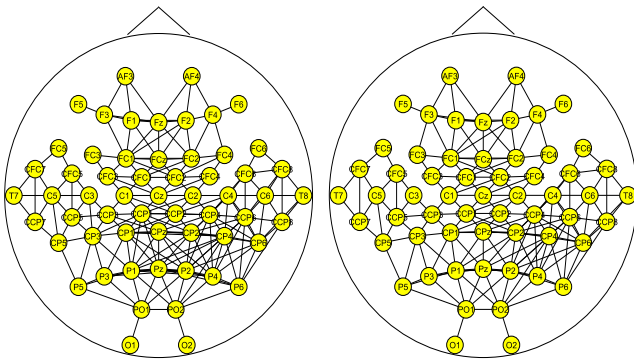
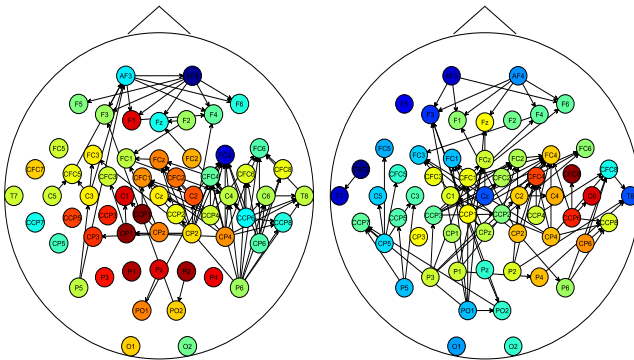


Fig. 1. L (left figure) and F (right figure) networks at mu band for subject a. The networks were calculated using the nonlinear RIM measure. Only edges with values above 0.8 are shown.



Vertex Level Metrics			Network L
Label	Strength	Efficiency	Hubbell
FC4	1.588	1.074	1.86
CCP6	2.012	1.893	1.377
FC6	1.233	1.161	1.268
CFC4	1.418	1.11	1.249

Vertex Level Metrics			Network Le
Label	Strength	Efficiency	Hubbell
Cz	0.015	0.02	1.08
CCP3	0.018	0.023	0.979
C1	0.018	0.019	0.976
C2	0.022	0.022	0.966

Fig. 2. **Above:** Network I minus L (left figure) [resp. I minus F (right figure)] at mu band for subject a. The networks were calculated using PDC. The color of a vertex shows the (average) PSD of state L (resp. F). Red colors correspond to higher values than blue colors. **Below:** Ranking of vertices of network I minus L (resp. I minus F) according to Hubbell's centrality index.

L (resp. I minus F), according to Hubbell's centrality, are relevant to state L (resp. F) (see the tables of Fig. 2).

## V. CONCLUSIONS AND FUTURE WORK

**Conclusions:** We created a Java application called BrainNetVis which is suitable for studying brain functional networks. The program runs as an application or it can be called as a function from Matlab. We describe most of the terminology and ideas behind this program with a case study of motor imagery. Using this program we found that at sensors space it is hard to distinguish between the left and foot imagery states using the corresponding synchronization networks because these networks are dominated by irrelevant edges. We propose to construct the difference network L minus I (resp. F minus I) as well as the difference network I minus L (resp. I minus F). By visualizing the difference networks we found that networks I and L (resp. I and F)

differ in interhemispheric edges and close to the left hand (resp. foot) area of the sensorimotor cortex.

**Future Work:** Our effort with the development of BrainNetVis program will continue. In the next version of BrainNetVis we plan a) to implement community structure (graph clustering) algorithms as well as graph drawing algorithms that display the community structure and b) to extend its functionality to series of networks in order to study the dynamics of functional networks.

## VI. ACKNOWLEDGMENTS

The authors wish to thank the Berlin BCI group for providing the EEG data set<sup>1</sup> and L. A. Baccalá, K. Sameshima and D. Y. Takahashi for providing the matlab code for PDC<sup>2</sup>.

## REFERENCES

- [1] K. J. Friston, "Functional and effective connectivity in neuroimaging: A synthesis," *NeuroImage*, vol. 2, pp. 56–78, 1994.
- [2] B. Blankertz, G. Dornhege, M. Krauledat, K.-R. Müller, and G. Curio, "The non-invasive Berlin braincomputer interface: Fast acquisition of effective performance in untrained subjects," *NeuroImage*, vol. 37, pp. 539–550, 2007.
- [3] Z. Koles, "The quantitative extraction and topographic mapping of the abnormal components in the clinical eeg," *Electroencephalography and Clinical Neurophysiology*, vol. 79, pp. 440–447, 1991.
- [4] F. Mitschke, "Acausal filters for chaotic signals," *Phys. Rev. A*, vol. 41, no. 2, pp. 1169–1171, 1990.
- [5] F. Takens, "Detecting strange attractors in turbulence," in *Dynamical Systems and Turbulence*, ser. Lecture Notes in Mathematics, vol. 898, 1981, pp. 366–381.
- [6] R. Q. Quiroga, A. Kraskov, T. Kreuz, and P. Grassberger, "Performance of different synchronization measures in real data: A case study on electroencephalographic signals," *Phys. Rev. E*, vol. 65, no. 4, p. 041903, 2002.
- [7] L. A. Baccalá and K. Sameshima, "Partial directed coherence: a new concept in neural structure determination," *Biological Cybernetics*, vol. 84, no. 6, pp. 463–474, 2001.
- [8] T. Mima, T. Matsuoka, and M. Hallett, "Functional coupling of human right and left cortical motor areas demonstrated with partial coherence analysis," *Neuroscience Letters*, vol. 287, no. 2, pp. 93–96, 2000.
- [9] V. Latora and M. Marchiori, "Efficient behavior of small-world networks," *Phys. Rev. Lett.*, vol. 87, no. 19, p. 198701, 2001.
- [10] C. H. Hubbell, "An input-output approach to clique identification," *Sociometry*, vol. 28, p. 377399, 1965.
- [11] B. Zhang and S. Horvath, "A general framework for weighted gene co-expression network analysis," *Statistical Applications in Genetics and Molecular Biology*, vol. 4, no. 1, 2005.
- [12] M. E. J. Newman, "Assortative mixing in networks," *Phys. Rev. Lett.*, vol. 89, no. 20, p. 208701, 2002.
- [13] C. C. Leung and H. F. Chau, "Weighted assortative and disassortative networks model," *Physica A*, vol. 378, no. 2, pp. 591–602, 2007.
- [14] V. Sakkalis, V. Tsiaras, M. Zervakis, and I. G. Tollis, "Optimal brain network synchrony visualization: Application in an alcoholism paradigm," in *IEEE EMBS*, 2007, pp. 4285–4288.
- [15] E. R. Gansner, Y. Koren, and S. North, "Graph drawing by stress majorization," in *GD 2004*, ser. LNCS, vol. 3383, 2005, pp. 239–250.
- [16] Y. Koren and A. Cviril, "The binary stress model for graph drawing," in *GD 2008*, ser. LNCS, vol. 5417, 2009, pp. 193–205.
- [17] A. A. Ioannides, "Dynamic functional connectivity," *Current Opinion in Neurobiology*, vol. 17, pp. 161–170, 2007.
- [18] C. Calmels, M. Hars, P. Holmes, G. Jarry, and C. J. Stam, "Non-linear eeg synchronization during observation and execution of simple and complex sequential finger movements," *Experimental Brain Research*, vol. 190, pp. 389–400, 2008.
- [19] G. Florian, C. Andrew, and G. Pfurtscheller, "Do changes in coherence always reflect changes in functional coupling?" *Electroenceph. Clin. Neurophysiol.*, vol. 106, no. 1, pp. 87–91, 1998.

<sup>1</sup>[http://ida.first.fraunhofer.de/projects/bci/competition\\_iv/](http://ida.first.fraunhofer.de/projects/bci/competition_iv/)

<sup>2</sup><http://www.lcs.poli.usp.br/~baccala/pdc/>